Volume 16
Number 11
21 March 2020
Pages 2633–2874

Soft Matter

rsc.li/soft-matter-journal

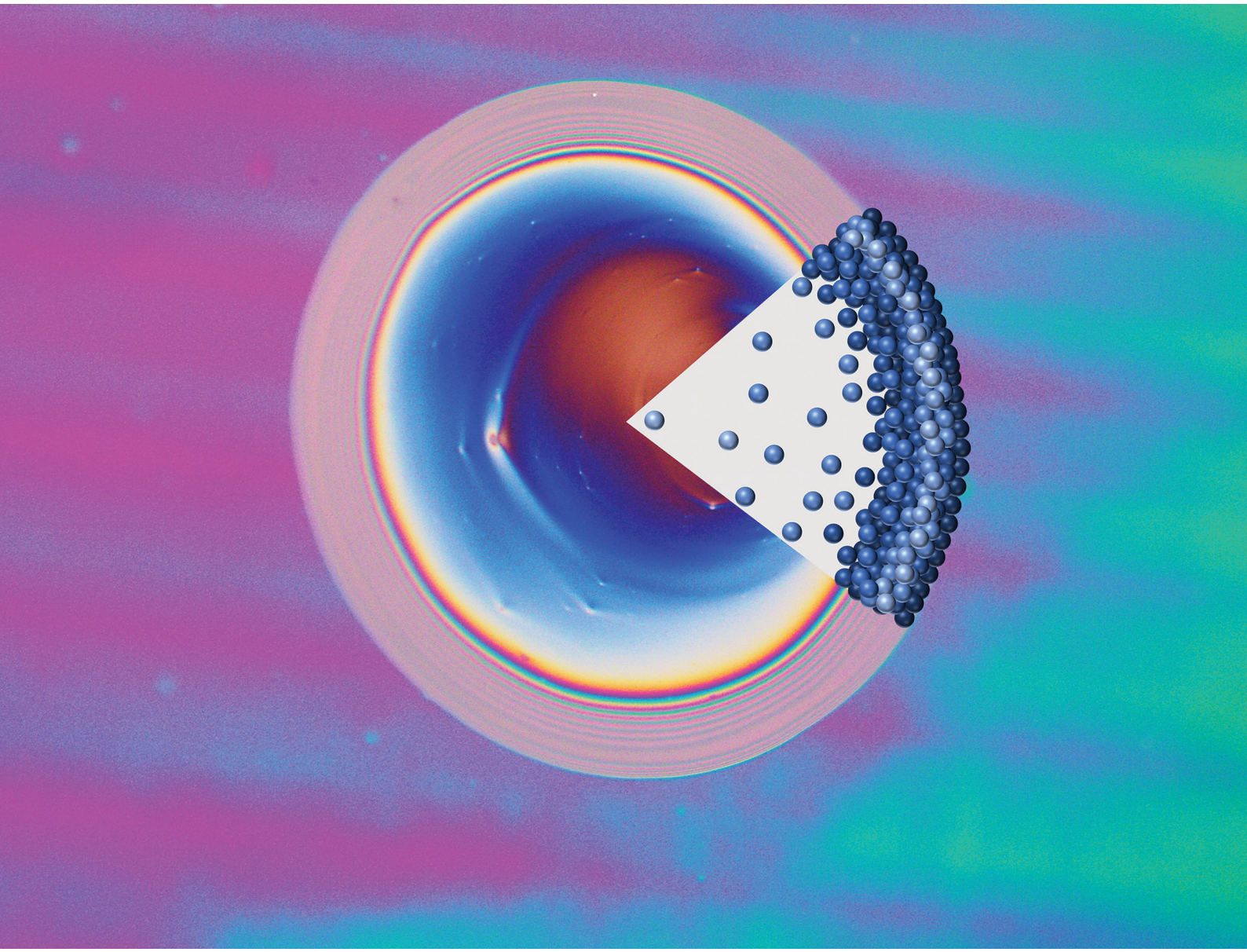

ISSN 1744-6848

ROYAL SOCIETY OF CHEMISTRY

PAPER
Sabina Islam and Orlin D. Velev
Mechanism and control of "coffee-ring erosion" phenomena in structurally colored ionomer films

Soft Matter

PAPER

Cite this: *Soft Matter*, 2020, **16**, 2683

Mechanism and control of "coffee-ring erosion" phenomena in structurally colored ionomer films†

Sabina Islam and Orlin D. Velev *

Received 15th December 2019,
Accepted 28th January 2020

DOI: 10.1039/c9sm02457c

rsc.li/soft-matter-journal

Ionomer polyesters have polymer backbones functionalized with charged groups that make them water-dispersible. Despite the widespread use of ionomer polymers in environmentally friendly coatings without volatile organic solvents, the fundamental understanding of their film formation properties is still limited. In the study, we deposited polyester nanofilms of brilliant structural colors and correlated the macroscale optical properties to the microscale thickness of the thin films. We found that sessile water droplets deposited on these films drive the formation of a rich variety of structures by an evaporation-induced effect of "coffee-ring erosion". The ionomers spontaneously get partially re-dispersed in the form of nanoparticles in the sessile droplets and driven by convective evaporation flows, become redistributed in multiple colorful ring patterns. By using the structural colors as means to follow the polymer redistribution, we characterized further the coffee-ring patterns and found that the generated patterns are dictated by polymer composition but are mostly independent on molecular weight. As expected by colloidal theory, this phenomenon was suppressed in presence of electrolytes. Furthermore, we show that the integrity of these thin polyester films can be significantly improved by thermal densification without any further chemical curing.

Introduction

Applications of traditional solvent-based polymer coatings lead to high emissions of volatile organic compounds, one of the major reactants causing the formation of toxic, ground-level ozone. Water-based polymers including, *e.g.*, waterborne polyurethanes, polyester dispersions, and polyacrylate emulsions have high potential as substitutes for organic solvent-borne systems for painting, adhesive, and coating applications not only because of their low environmental impact, but also for their low cost.[1–6] Polyesters are one of the most common classes of polymers with superior mechanical, optical, and processing characteristics. In order to use such polyester systems into waterborne formulations, a small fraction of functional monomers with ionic moieties can be incorporated into the polyester backbone, allowing the polyester resins to be directly dispersed in water. One class of common industrial polymers in this new generation of waterborne systems are sulfopolyesters, where an aromatic sulfonated monomer is incorporated as the ionic group. In our previous study, we characterized the colloidal interactions of sulfopolyester dispersions using various light scattering techniques and a range of commercial sulfopolyesters as a model system.[7] We found that, based on the molecular weight and ionic monomer composition, hundreds of polyester molecules undergo self-assembly in water to form nanoparticles where the aggregation is determined by a critical surface-charge density of the nanoparticles. Once aggregated in water, these soft colloidal nanoaggregates behave like traditional hard colloids as the interparticle interactions and phase properties in water are governed by classic DLVO interactions.[7] In the present study, we investigate the correlation between the colloidal properties of sulfopolyesters and the stability of the dried nanofilms in presence of water as a corrosive agent.

Polymer composition, molecular weight, and particle size govern the essential film parameters such as glass-transition temperature (T_g) and minimum film formation temperature (MFFT) for optimum film performance. While a high T_g ensures increased hardness and resistance of the film, it is also associated with increased MFFT, which means that longer process times or higher process temperatures are required during application. As a result, conventional latex-based waterborne systems with high T_g inevitably require the addition of volatile coalescent agents or plasticizers in order to promote film formation at ambient temperature.[8–10] Substantial volume of research on the drying processes of emulsion-based latex systems has been reported to explain the mechanism of transformation from colloidal dispersions to a continuous polymer films.[11,12] The widely accepted model for this process is divided

Department of Chemical and Biomolecular Engineering, North Carolina State University, Raleigh, NC 27695, USA. E-mail: odvelev@ncsu.edu

† Electronic supplementary information (ESI) available. See DOI: 10.1039/c9sm02457c

into three essential stages, namely, (1) drying: water evaporation leading to close-packed structure, (2) deformation: filling up of void space by hexagonal deformation of particles, and (3) coalescence: fusion of particle boundaries by polymer interdiffusion to form a continuous film.[8,13] Unlike traditional latex polymers, waterborne polyurethane and polyester dispersions do not require addition of coalescent agent. Moreover, these colloidal systems form optically smooth and glossy films when applied to a surface with a short drying time at room temperature. This is attributed to extremely small particle size distribution and the effective plasticization of the nanoparticles by water.[9,14] However, since water is essentially the plasticizer for coatings of waterborne polyester nanoparticles, it is crucial to understand the structural integrity of the deposited coatings upon exposure to an aqueous environment.

Structural color is a natural optical effect originating from the physical interaction of light with nanostructures such as butterfly wings and natural opals.[15] Structural color offers numerous benefits over pigment-based colors, such as more vibrant color formation, resistance to photobleaching, and avoidance of environmental toxicities associated with pigmentation.[16,17] Colloidal particles on the micro- and nanoscale offer one of the most versatile and inexpensive bottom-up methods to achieve required architecture for the emergence of the structural color of purely physical origin.[17,18] As a result, the research on this type of chromophore-independent colors of films from small particles is of significant interest to industry and academia.[16–25] The optical properties of films from colloidal nanoparticles have been tailored to develop various colorimetric sensing materials,[21,23] photonic papers,[26,27] next generation color printing technologies,[20,24] and superhydrophobic and superhydrophilic surfaces.[28,29]

We took advantage of the structural color of nanofilms composed of polyester nanoparticles to correlate their colloidal interactions to the stability of the deposited coatings. We first investigated the origin of structural color of nanofilms made of polyester dispersions. We then found that upon depositing sessile water drops on the dried polyester films, the uniformity of the nanofilm changed as a result of water evaporation. We present a model for such evaporation-induced water damage of the polyester films. We then examined how varying the chemical structure and molecular weight of the sulfopolyesters affects the interaction of water with the deposited film and investigated strategies for mitigating such water damage. The findings of this study may help in designing next-generation waterborne polymers for maximum film performance.

In this study, we used sulfopolyesters of varying composition of two diacids and two diols, namely, isophthalic acid (IPA), 5-sodiosulfoisophthalic acid (SSIPA), diethylene glycol (DEG), and 1,4-cyclohexanedimethanol (CHDM). The general structure of the sulfopolyesters is shown in Fig. 1a and their chemical composition is given in ESI† Table S1. In the previous study on the colloidal dispersion properties of these sulfopolyesters, we measured the nanoparticle size in water using dynamic light scattering (DLS). The DLS data showed the sulfopolyesters form self-assembled nanoparticles in the range of 25–96 nm of average diameter (Fig. S1, ESI†).[7]

Results

Colorful nanofilm from polyester dispersion and origin of the optical color

For most of the film formation study, we have used convective film deposition, which is a very simple, rapid, and scalable technique for controlling film structure and thickness. The process is governed by solvent evaporation from a thin liquid film wetting a substrate where the solvent evaporation drags dispersed particles into the drying region and deposits them in uniform film (Fig. 1b).[30] We used 30 wt% dispersions for depositing the sulfopolyesters films. As the polyester nanoparticles were captured in the growing film, compact and uniform coatings were formed (Fig. 1b). The polymer films were brilliantly colored when deposited on a Si wafer substrate and the visualized color was dependent on the viewing angle. This structural color arises from the interaction of light with ordered micro/nanostructures. Natural structural color can be of two kinds depending on the surface feature: periodic anisotropic or isotropic nanostructure.[31] To understand the origin of the color of the sulfopolyester films, we first utilized atomic force microscopy (AFM) to visualize the nanostructure of the film. We found that the polymer film was extremely uniform and smooth with a root mean square (RMS) roughness of 0.41 nm (Fig. S2, ESI†), indicating absence of periodic anisotropic features. Next, we measured the thickness of the film using AFM along the edge of the film and determined it to be around 400 nm, which confirmed the deposited film was indeed of nanoscale thickness (Fig. 1c).

The structural color originating from isotropic nanostructure strongly depends on the thickness of the film.[32] To check the validity of this correlation, we varied the film thickness by diluting the polymer dispersions. The color completely disappeared when a 10 wt% polymer dispersion was used instead of 30 wt% while keeping all other deposition parameters (*i.e.*, deposition speed, temperature, humidity) unchanged (Fig. 1d). The thickness of the film resulting from a 10 wt% polymer dispersion was measured to be 30 nm. Next, to increase the film thickness, we deposited a second layer of polymer film on top of the first one. Again, the structural color disappeared when the second layer of the polymer film was deposited on the first polymer layer that was colorful (Fig. 1d). Thus, the structural color of the sulfopolyester films was shown to be strongly dependent on the thickness of the nanofilms, as the color disappeared if the film was too thin or too thick. This evidence suggests that the structural color is a result of thin film interference as commonly displayed in soap bubbles.

Constructive thin film interference is described by Bragg's law,[33] which takes into account that when an electromagnetic wave interacts with a film's surface, a part of the radiation is immediately reflected from the top surface and another part by the bottom one. The extra path travelled makes the two wavelengths to interfere constructively or destructively depending on the phase difference when the film thickness is comparable to the wavelength. To an observer, the film will appear of color corresponding to the constructive interfering wavelength.

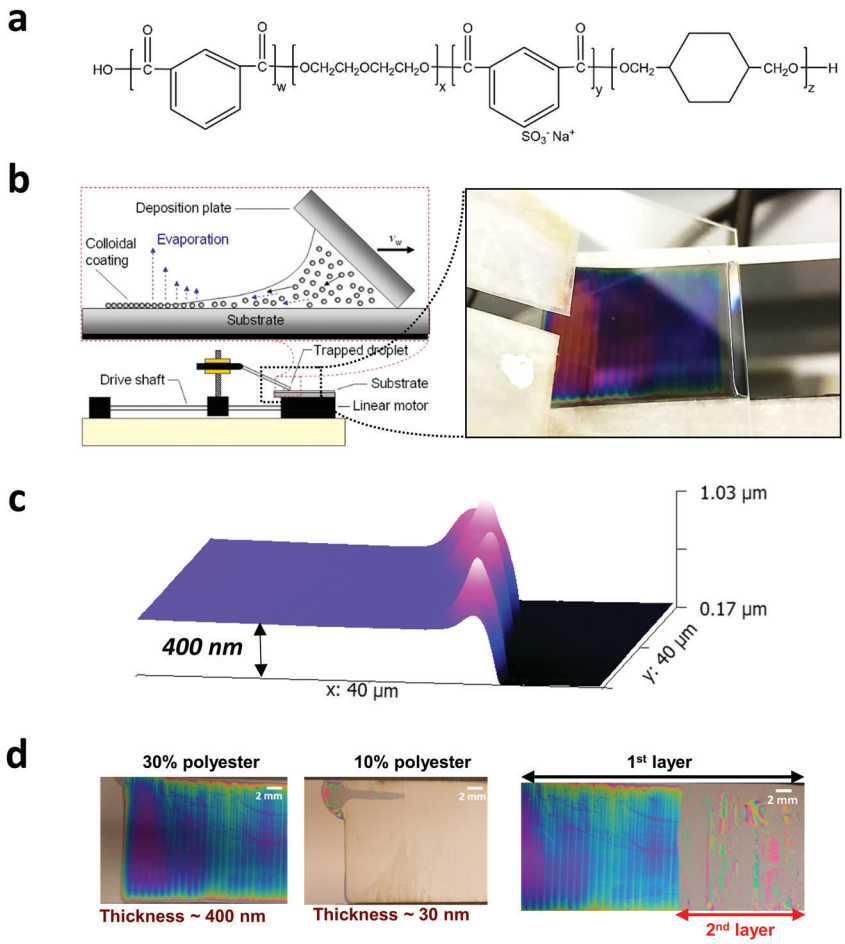

Fig. 1 Colorful nanofilm from polyester dispersion (a) the general structure of the sulfopolyesters where *x* and *z* represent % glycols (*i.e.*, DEG and CHDM respectively) and *w* and *y* represent % diacids (*i.e.*, IPA and SSIPA respectively). (b) Structural color emerges as film is being formed due to solvent evaporation from the polyester dispersion *via* the convective assembly method. (c) AFM study on the polyester film allowing to measure its thickness. (d) Thickness-dependent structural color formation where the structural color disappears if the thickness is too low (10% polyester) or too high (a 2nd layer of polymer film was cast on the half of the substrate having the 1st layer of the polymer film using the same deposition condition).

For the sulfopolyester nanofilms, Bragg's law is represented by eqn (1).

$$2h \sin\theta = \frac{m\lambda}{n_{\text{polyester}}} \quad (1)$$

where h is the thickness of the film (*i.e.*, spacing between the reflecting planes), θ is the angle between the incident ray and plane of scattering (*i.e.*, 90° if film is viewed from top), $n_{\text{polyester}}$ is the refractive index of the polymer, λ is the wavelength for which constructive interference takes place, and m is the integer value of diffraction order. The electromagnetic wave undergoes phase shift based on the difference of refractive indices of the two interfaces. Since $n_{\text{polyester}}$ is higher than n_{air} and n_{Si} is higher than $n_{\text{polyester}}$, both reflected waves will experience same phase shift of π (Fig. 2a).

Next, in order to correlate the structural color to small variations of the thickness of the film, we fabricated polyester films with different thicknesses using spin-coating, which offers stringent control of the film thickness. In this way, the coloration of the deposited films could be altered by manipulating the spin-coating speed. Three films were fabricated of violet, yellow, and green color when viewed from the top. Their thicknesses were measured independently using ellipsometry. By using the refractive index and measured thickness information, we calculated the theoretical wavelength (λ) at which constructive interference should occur using eqn (1) for $\theta = 90°$ and $m = 1, 2, 3,$ or 4 and found that m should be 2 in this case, as other m values result in a wavelength number that is out of the range of visible wavelengths (Table S3, ESI†). Finally, we reproduced the theoretical colors corresponding to the calculated interference wavelength of visible light. We found that the actual colors on the films match quite accurately the predicted theoretical colors, which confirms our hypothesis that the bright structural colors on the polymer nanofilm are a result of constructive thin film interference (Fig. 2b). That correlation of structural color of the film to the thickness suggests that we can use these brilliant colors as measure of film thickness.

Coffee-ring erosion by water evaporation

Since these polyester nanofilms are made of waterborne nanoparticles, we aimed to observe how their wetting by pendant

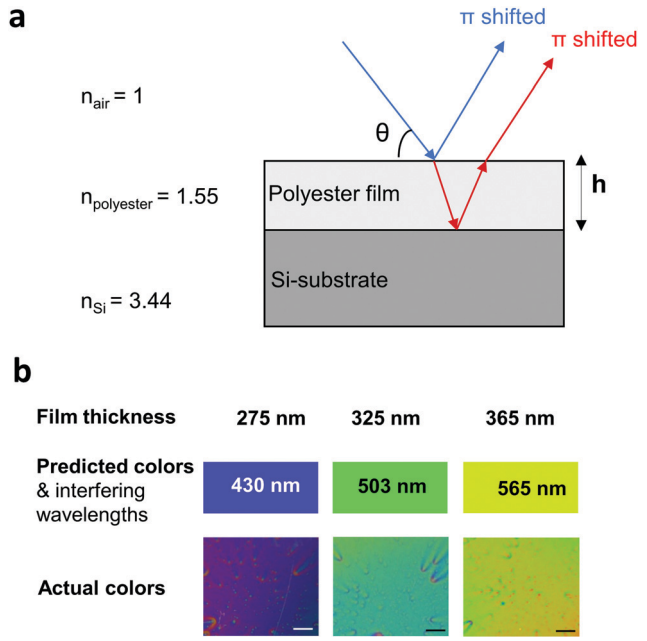

Fig. 2 Structural color emergence from thin film interference. (a) Model for constructive interference on thin polymer film. (b) Predicted theoretical colors for constructive thin film interference from the thickness values obtained from ellipsometry study match the actual structural colors of the three films. Scale bar is 1 mm.

droplets will affect film stability and uniformity. If the film was completely water-resistant, there would be no change in structural color after the water droplet evaporates. However, as can be seen in Fig. 3, a new set of fascinating colored patterns emerged as a result of sessile water droplet deposition and evaporation. The wetting and evaporation of water is causing the nanofilm to rearrange as shown by colored rings of differing thicknesses. The water damage created a distinct pattern with a sharply defined edge, concentric colorful rings, and a black or deep blue region near the center (Fig. 3b). The multiple colorful rings indicated the appearance of different thicknesses of the polyester film. Such a nonuniform film rearrangement could happen if the nanoparticles in the film had re-dispersed in the droplet and had been carried to the edge of the droplet. This drying pattern appears broadly similar to the "coffee-ring effect" where evaporation of solvent from a liquid drop with suspended particles on a solid surface leads to deposition of rings of piled-up particles along the edge of the original liquid drop.[34] It appears that the polyester nanoparticles re-disperse to some extent, and as the solvent evaporates, the outward radial convective flow carries them to the periphery of the pinned drop. As a result, a thicker ring of suspended particles is deposited at the perimeter of the dried droplet. Since the water evaporation induces a permanent erosion in the film in a coffee-ring pattern, we named this phenomenon "coffee-ring erosion."

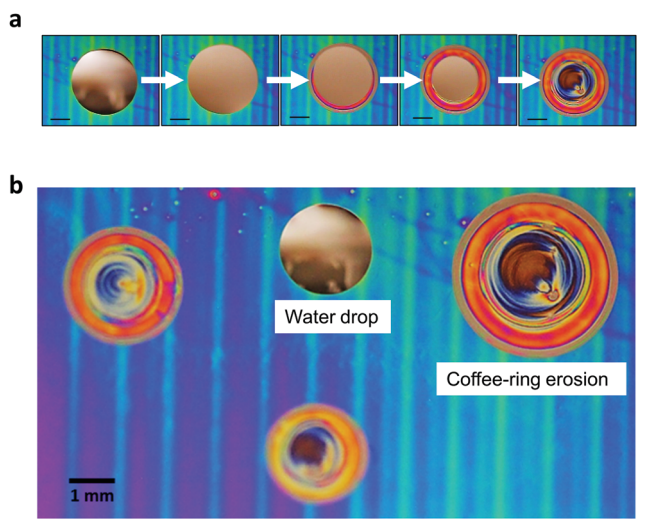

Fig. 3 Coffee-ring erosion of a thin polyester film. (a) Time lapse snapshots of film rearrangement as a result of water evaporation leading to new structural color pattern indicating different thickness of films following erosion. (b) The thin black region in the middle of the erosion area indicates the presence of effects similar to "coffee-ring" formation in drying droplets.

A simple calculation using eqn (1) shows that the thickness of the polyester nanofilm needs to be at least 130 nm in order to allow constructive interference of visible wavelength range to take place. Thus, the black region at the center of the droplet is evaluated as less than 130 nm thick. To check the thickness of the erosion profile, we performed a profilometry study on the erosion pattern after water droplet evaporation (Fig. 4). The edge of the rings was at least 700 nm higher than the center, whereas center was 550–600 nm thinner than the bulk film. Based on the orange structural color, the thickness of the bulk film was calculated to be 598 nm, which is similar to the film thickness measured by ellipsometry. This result suggests that the polyester nanoaggregates at the center of the erosion pattern migrated to the edge due to the outward radial capillary flow of water. It confirms that the multiple-ring formation at the periphery of the evaporating water droplet evaporation is indeed caused by a coffee-ring type of convective re-distribution.

Effect of composition of the damaging liquid

The classic coffee-ring phenomenon is known to be affected by the presence of electrolytes[35] or surfactants.[36,37] To check how the colloidal interactions between the polyester nanoparticles affected by such additives influences the coffee-ring erosion profile, we investigated the role of sodium chloride (NaCl), cetyltrimethylammonium bromide (CTAB) and sodium dodecyl sulfate (SDS) solutions as damaging liquids (Fig. 5). In the presence of NaCl, the coffee-ring effect was suppressed as the concentric ring structure was absent (Fig. 5a). This ring suppression effect in presence of electrolyte was further verified using profilometry, showing that the height profile was rather uniform along the edge of the droplet (Fig. S3, ESI†). Similarly, the addition of surfactants also affected this capillary interaction-driven erosion. The pattern formation in the case of the cationic surfactant, CTAB, *vs.* the anionic surfactant, SDS, was completely different (Fig. 5b and c). In the case of CTAB, the dried pattern was opaque, uniform and devoid of any centered ring, whereas in presence of SDS, the dried pattern

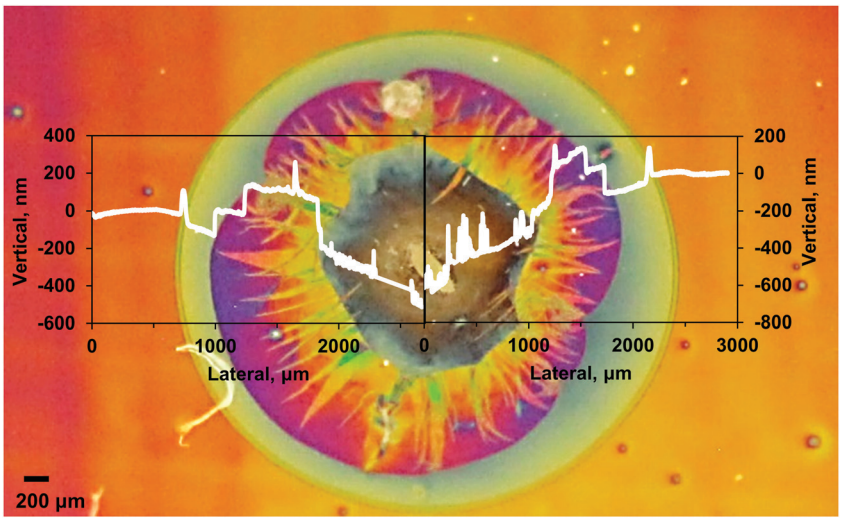

Fig. 4 Damage profile resulting from "coffee-ring erosion". The thickness profile obtained *via* profilometry is overlaid on the color image of the damaged polyester film. Both show that the edge is at least 700 nm thicker compared to the center of the erosion profile indicating coffee-ring-like redistribution phenomenon.

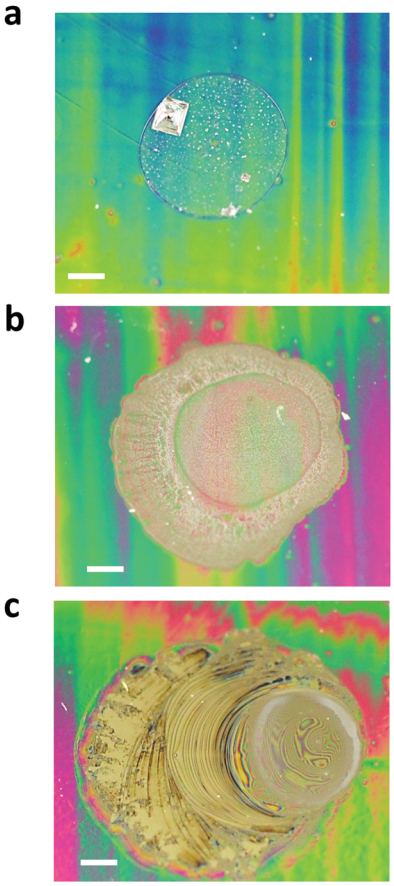

Fig. 5 Effect of electrolyte or surfactants on the erosion profiles of polyester nanofilms. The erosion profile depends on the composition of the damaging liquid. Coffee-ring erosion is suppressed in case of (a) 1 M NaCl solution, whereas solutions of (b) 10 mM CTAB and (c) 10 mM SDS in the droplet creates a dramatically different damage structure on the polyester film. Scale bars indicate 1 mm.

consisted of numerous black rings. In our previous work, we demonstrated that the sulfopolyester nanoparticles are electrostatically stabilized and negatively charged, being ornamented with the negative surface charge group SSIPA.[7] The variety of erosion profiles generated in response to different additives in the damaging liquid indicates that the redispersion and redistribution of the polyester nanoparticles depends on the colloidal interactions between the nanoparticles.

Effect of the nature of ionic groups

The sulfopolyesters were molecularly designed to incorporate a permanently charged group, SSIPA, attached to the backbone of the polymers in order to render dispersibility in water. While these sulfopolyesters form stable dispersions readily without any additional cosolvent, an inherent difficulty arises as certain applications require coatings and materials with high water resistance. An alternate way to disperse waterborne polyesters is to incorporate pH-sensitive charged groups such as –COOH in the polymers. These carboxylated polyesters can be dispersed in water using volatile amine-base compounds so that once the film is formed and dried, the amines escape, leaving more resistant dried films. To check this hypothesis, we made a film from a polyester stabilized by pH dependent –COOH groups (*i.e.*, polyester 9 in Table S2, ESI†) and performed the same water-droplet erosion test. As in Fig. 6, the water damage was completely suppressed when the charged group was changed from the permanent $-SO_3Na$ to the pH dependent –COOH. This result confirms that the re-dispersibility of the polyester nanoparticle in water droplet is the key component for such coffee-ring erosion of waterborne polyester films.

Mechanism of coffee-ring erosion by water

As explained, we hypothesize that the polyester nanoparticles re-disperse within the water droplet medium for the coffee-ring

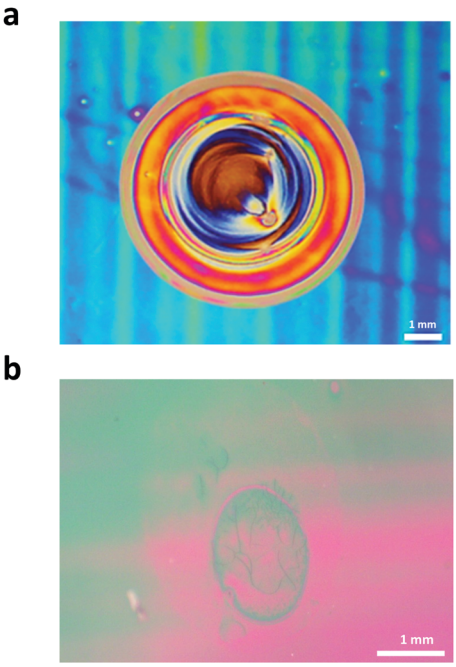

Fig. 6 Effect of nature of ionic molecular group on the erosion profiles on thin polyester film. The erosion profile depends on the nature of the ionic groups of the polyester. (a) Coffee-ring erosion of thin film of polyester 7 with permanent charge group $-SO_3Na$ whereas (b) such damage is absent for polyester 9 with pH-dependent charge group –COOH. The pH of the dispersion was 7.5.

erosion phenomenon to occur. We illustrate the step-by-step mechanism of such film damage in the schematic in Fig. 7. The polyester dispersion forms uniform nanofilm upon drying. When the water droplet is deposited on top of this dry film, the polyester molecules in contact with water re-disperse as nanoparticles again. As the water droplet evaporates, the radial outward capillary flow drags the nanoparticles toward the edge and the polyester film is redistributed. If this hypothesis was correct, the re-dispersed nanoparticle will have the same size as the original polyester dispersion. To check that, we performed DLS to compare the particle size in step (a) and (d). Indeed, the particle size distribution was almost the same for the original dispersion and after redispersion in the damaging water droplet (Fig. S4, ESI†).

Stability of dried polyester dispersions

The water evaporation-induced coffee-ring erosion profiles of the polyester nanofilms are a result from both nanoparticle redispersion and water evaporation. To understand the interaction of water droplets with these polyester films in further detail, we first aimed to understand the simple droplet drying behavior of droplets from aqueous polyester dispersions (Fig. S5, ESI†). In order to systematically study the drying process of the polyester nanoparticles, we first checked the effect of polymer concentration on the coffee-ring profile with polyester 7. We found that over the wide range of polyester concentration (*i.e.*, 0.01–8%), the coffee-ring pattern was similar and that the majority of the polymer mass was deposited at the periphery as a single, colorless ring, whereas there was thin film deposition inside the pattern (Fig. S6a, ESI†). The thickness of the nanofilm inside the patterns increased proportionally with the polymer concentration (Fig. S6b, ESI†). As a result, the structural color of thin films inside the pattern was also a function of polymer concentration, where the structural color disappeared if the film thickness was too low or too high. A simple phase diagram in Fig. 8a depicts the correlation of the structural color to the concentration of the polymer dispersion.

We then checked the effect of droplet volume on the drying profiles. As demonstrated in Fig. 8b, the area of the deposited coffee-ring patterns increased with the polymer concentration. To understand these effects in detail, we performed contact angle measurements. We found the drying of these polyester dispersions occurred under conditions of constant contact area as expected for coffee-ring patterns (Fig S7b, ESI†).[38] The contact angle of the dispersion droplet decreased with increasing polymer concentration (Fig. S7c, ESI†). This can be explained with the surface activity of these polyester dispersions. As the polyester concentration increases, the surface tension at the air–liquid interface decreases. As a result, the contact angle decreases, which leads to a larger contact area of the dried deposit. On the other hand, when the droplet volume was varied, the contact angle did not change, and the droplet height increased as expected (Fig. S7d, ESI†). Therefore, the coffee-ring profile pattern did not change for different droplet volumes (Fig. 8b). These findings indicate that the final coffee-ring pattern is a tightly controlled by the contact angle and the polyester concentration in the droplet.

Next, we examined the effect of interparticle interactions on the coffee-ring profile of the dispersion droplets. Since the polyester nanoparticles are electrostatically stabilized, we suppressed their interaction by increasing the ionic strength with added electrolyte. As depicted in Fig. 9, the structural color of the inner film disappeared with increasing electrolyte concentration, which indicates a higher inner thin film thickness. Quantitatively, this phenomenon can be also expressed by measuring the surface fraction of the thick outer annulus region in comparison to the thin inner film region. We found that fraction of the outer annulus area compared to the inner film area decreased with increasing electrolyte concentration (Fig. 9). As the concentration of the electrolyte increases, electrostatic repulsion between the particles decreases, leading to aggregate formation within the droplet. These large aggregates constrict and ''jam'' the deposited structure, hindering the transport of the particles to the edge and suppressing in coffee-ring formation.[38]

Effect of polyester composition on the coffee-ring erosion

The sulfopolyesters are composed of two different glycols and two different acid groups where DEG and SSIPA are hydrophilic and IPA and CHDM are hydrophobic (Fig. 1a). To test which monomers are playing a key role in promoting water damage, we synthesized three controlled sets of polyesters: set-1 with varying glycol composition and constant acid composition; set-2 with varying acid composition and constant glycol composition;

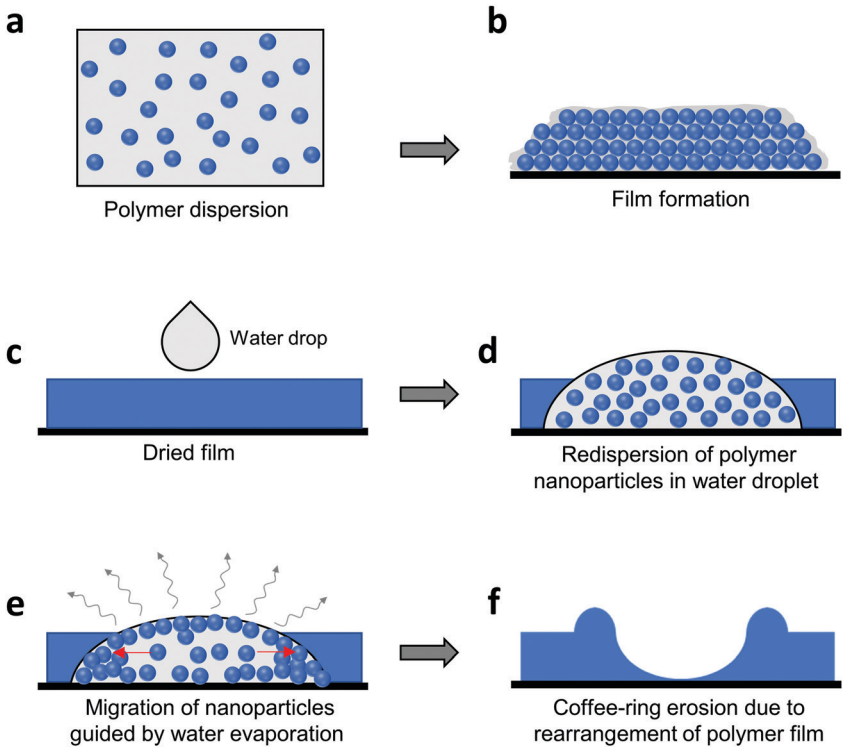

Fig. 7 Schematic of coffee-ring damage on polyester film. (a) Polyester dispersion is applied on the substrate; (b) uniform film is formed as dispersant water evaporates; (c) deposition of water droplet on the dried film; (d) polyester nanoparticles re-disperse in the sessile water droplet; (e) migration of nanoparticles to the edge of the droplet due to liquid convection as water evaporates; (f) coffee-ring erosion of polyester film as a result of water damage.

set-3 with varying molecular weight (MW) and constant acid and glycol composition. This allowed us to obtain polyesters with various solubility and colloidal properties.

We deposited water droplets on films from these polyesters and observed the erosion profiles (Fig. 10). The deep blue or black region at the center of the damage profile indicates the deepest erosion. Although area of damage was smaller, the damage was more severe on coatings with increased DEG (*i.e.*, the polar glycol group) or decreased CHDM (*i.e.*, the non-polar glycol group) content. The damaged area was almost the same for the various SSIPA compositions, however, the erosion increased with increased SSIPA. Surprisingly, the molecular weight (MW) had little effect on the coffee-ring erosion (Fig. S8, ESI†). This result indicates that the composition of the polyester determines the extent of such water evaporation induced erosion. One way to improve the water-resistance would be to tailor polyester compositions with less hydrophilic groups.

Finally, we investigated additional mitigation strategies for limiting water damage to these polyester films. We subjected the films to heat curing and performed the same water damage tests. We found that the water damage was greatly reduced for all conditions except the highest SSIPA composition (Fig. 11). The water resistance was generally improved for polyesters of varying MW (Fig. S9, ESI†). Overall, since the polyester with the lowest SSIPA composition is hard to disperse and the highest SSIPA composition leads to severe coffee-ring erosion, the polyesters should be designed to have a moderate SSIPA content to impart both rapid dispersibility to the polymer and greater water resistance to the resulting coating.

Discussion

Water-dispersible polymers have big potential for present and future sustainable clear and colored coating applications. For successful design and optimal functioning of waterborne coatings the polyester molecules need to be dispersible in water to obtain a stable dispersion, however, the resulting coatings made of the waterborne dispersion should exhibit water resistance. Therefore, it is crucial to understand the film formation properties of these waterborne systems and their interaction with water for maximizing their utility in commercial applications.

The uniformity and stability of the coatings from waterborne aromatic polyesters was investigated by taking advantage of their optical properties. The dispersions made of sulfopolyester nanoparticles yielded uniform films of brilliant structural color. We used that structural color to measure film thickness by relating them *via* the interference theory. The change in the color of the polyester films was followed while depositing and evaporating water droplets on their surfaces. Films damaged after the droplet deposition displayed ring patterns of different colors which resembled the convective "coffee-ring" formation during droplet evaporation. Such coffee-ring distribution of particles is routinely encountered while drying suspensions in

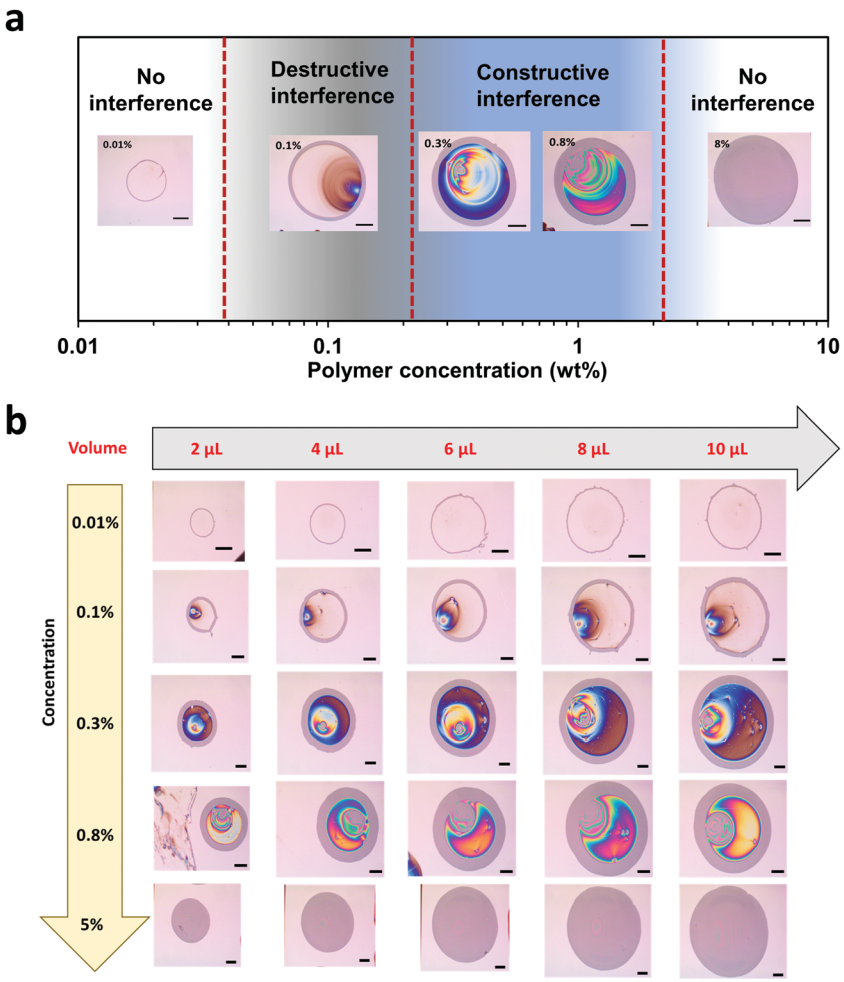

Fig. 8 Classical coffee-ring patterns formed during drying of sessile droplet polyester dispersions. (a) A simple phase diagram illustrating the effect of dissolved polymer concentration on droplet drying behavior shows that the coffee-ring pattern was common for a wide range of concentrations, whereas structural color appears within a particular concentration range. (b) The resulting coffee-ring profile is independent of droplet volume and dependent on the polymer concentration, which affects the contact angle of the deposited droplet. Scale bars are 1 mm.

thin film, coating, and printing processes.[39] However, the new element of our study is the use of coffee-ring phenomenon combined with structural color to investigate and analyze polymer film integrity. As water encounters the polymer film, the polyester gets re-dispersed as nanoparticles and guided by evaporation fluxes, gets re-deposited in a coffee-ring fashion at the periphery of the droplet. The classical coffee-ring formation from droplet evaporation results in positive elevation (increased thickness). In our system, the post-deposition water damage of the polyester films results in both positive and negative elevation during the erosion and evaporation-driven lateral polymer distribution (Fig. S10, ESI†), a phenomenon that we named "coffee-ring erosion."

The polyester films were not damaged when electrolytes were added in the water droplet (Fig. 5a). The presence of electrolytes prevents the nanoparticles from redispersion. The damage profiles were vastly different when ionic surfactants were introduced. In presence of a positively charged surfactant, CTAB, the damage profile was devoid of any peripheral ring and was rather opaque (Fig. 5b). The positively charged CTAB molecules may have aggregated the negatively charged polyester nanoparticles, thus preventing the coffee-ring erosion. On the other hand, the presence of negatively charged SDS molecules created dramatically different damage profiles full of many small ultra-thin black ring structures but devoid of a thick peripheral ring. This structure resembles the previously studied deposition profile of sulfonated polystyrene latex particles in presence of SDS.[37] The Marangoni flow generated by the presence of SDS molecules prevented deposition of the thick peripheral ring, whereas the multiple ultra-thin black rings resulted from repeated pinning and depinning of the contact line. Water erosion was also absent when the ionic nature of the polyester was changed from a permanent charge group of $-SO_3Na$ to a pH-dependent one –COOH (Fig. 6). These results indicate that the solubility and the interaction of the polymer with the damaging liquid agent is crucial for determining the erosion profiles.

The coffee-ring erosion of the polyester nanofilms is a complex outcome of nanoparticle redispersion in the liquid droplet and redistribution of the nanoparticles in a coffee-ring manner.

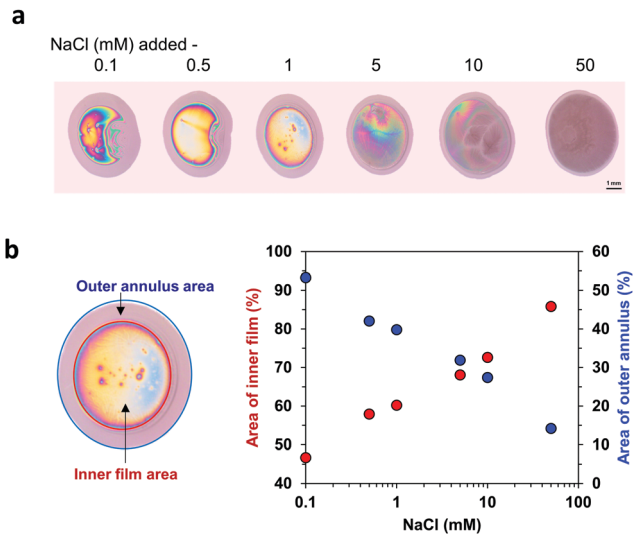

Fig. 9 Suppression of coffee-ring phenomenon in presence of electrolyte. (a) Sessile droplet drying profile of 0.7 wt% polyester with differing NaCl concentration shows that the structural color disappears with increasing electrolyte concentration, which indicates higher thickness of the inner film. Scale bar is 1 mm. (b) The area of the inner film increases with increasing electrolyte while the outer annulus area decreases showing coffee-ring suppression.

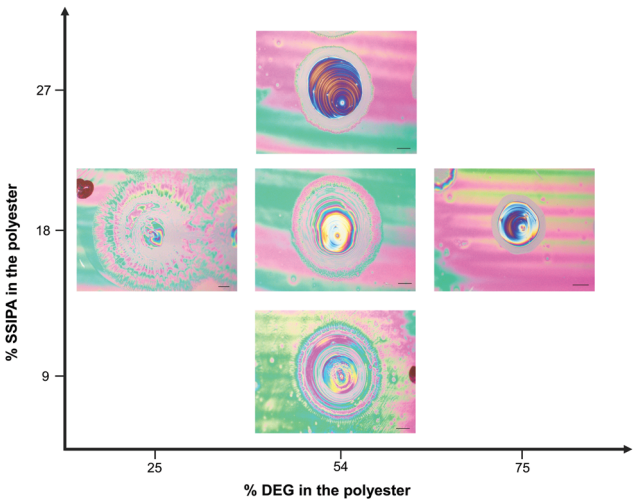

Fig. 10 Effect of polyester composition on coffee-ring erosion. Effect of acid composition denoted by %SSIPA in the *Y*-axis and the effect of glycol composition denoted by % DEG in the *X*-axis shows that coffee-ring erosion is more prominent for polyesters with higher %SSIPA composition. Scale bars = 1 mm.

The well-known coffee-ring phenomenon has been extensively studied by modulating the shape of the particles,[40] controlling the Marangoni flow of the solvent,[41] inducing rapid solvent evaporation at elevated temperature,[42] or by changing the interfacial properties in presence of surfactants.[37,43] The previous studies have been conducted with polystyrene latex of 0.5–1.3 μm in diameter, while we investigated the drying behavior of self-assembled waterborne nanoparticles of 20–50 nm in size. Therefore, we also characterized the drying behavior of

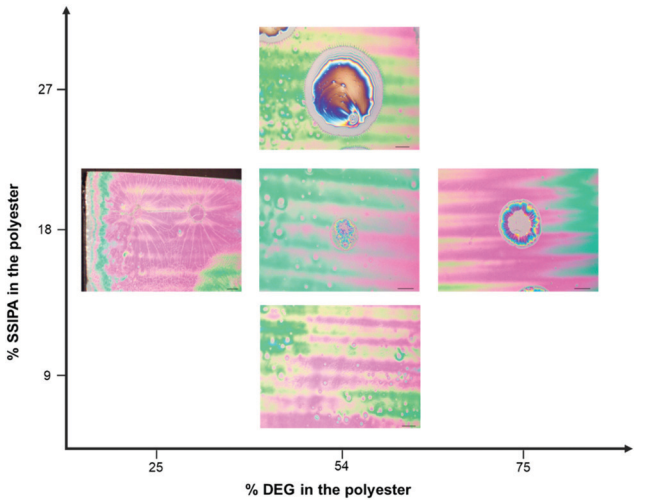

Fig. 11 Mitigation of coffee-ring erosion by heat-curing the films. In these experiments, the films were treated at 50 °C in an oven for 16 h before conducting the droplet test with water. Heat treatment of the polyester films of different composition mitigates the coffee-ring erosion for all compositions except for the highest %SSIPA composition. Scale bar indicates 1 mm.

sessile droplets as a function of polyester concentration, droplet volume and varying electrolyte concentration. The resulting coffee-ring profiles were independent of droplet volume but were strongly dependent on the polymer concentration (Fig. 8 and Fig. S6, ESI†). The structural color of the inner film was black or blue for the lowest polymer concentration indicating extremely thin, nanoscale inner film. Since the contact angle was determined by the polymer concentration, but was independent of the droplet volume, we conclude that the final coffee-ring pattern was governed by the contact angle of the deposited droplet. Additionally, the presence of electrolytes suppressed the coffee-ring formation as expected by the colloidal interactions leading to aggregation.

The composition of the polyesters played a key role in determining the extent of water damage. The erosion was more severe with increasing composition of both hydrophilic monomers, DEG and SSIPA (Fig. 10). The smallest molecular fraction of hydrophilic groups required for proper dispersibility as well as uniform film formation were at least 9/54 (% SSIPA/DEG). In case of such small hydrophilic group fraction, it takes longer time for the polyester to disperse in pure water. If the fraction of hydrophilic groups is lower, then an organic co-solvent will be needed in order to disperse the polyester.[7] However, films from such polyesters are prone to developing cracks (result not shown). The degree of the damage was related to the solubility of the polyester where the highly soluble one caused single coffee-ring profiles, the moderately soluble polyester showed multiple rings, and the polyester with lowest fraction of soluble groups resulted in a gel pile-like incomplete damage profile. We summarily illustrate these phenomena in Fig. 12. The single coffee-ring structure with biggest erosion depth for the highly soluble polyester resembles the deposition pattern observed for sessile droplet test in Fig. 8. This suggests that

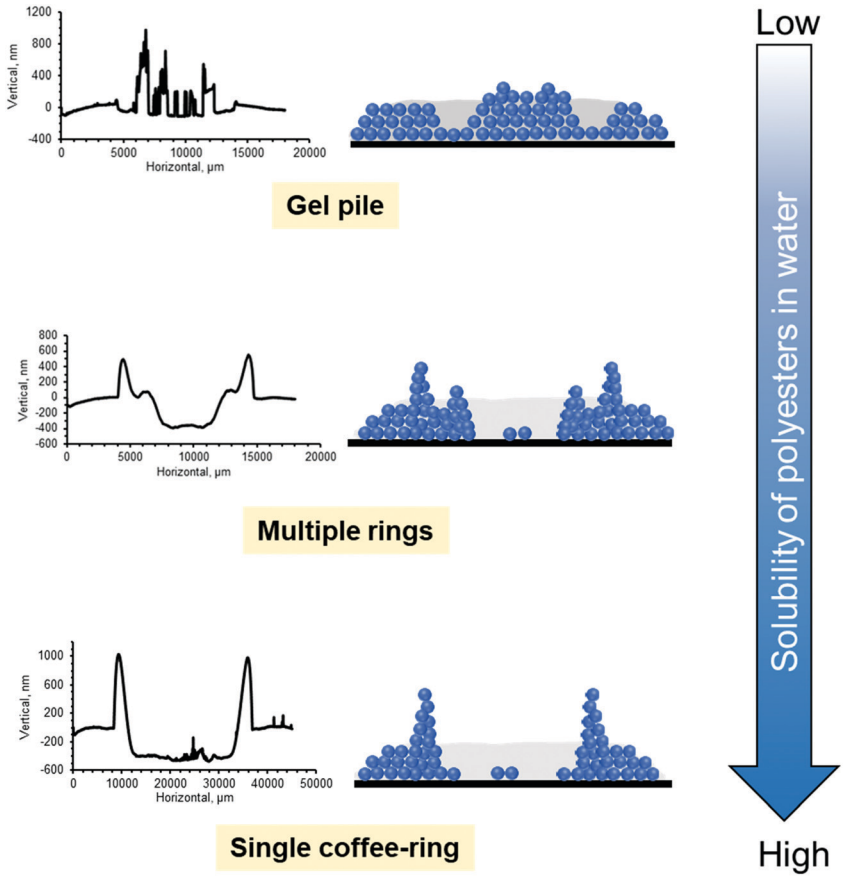

Fig. 12 Varying erosion profiles based on polyester solubility. The solubility of the polyesters determines the degree of erosion damage. Profilometry reveals the damage profile to be in the form of single coffee ring for highly soluble polyester, multiple rings for moderate solubility and "gel pile" deposition pattern for lowest solubility (compare with Fig. 10).

all of the polymer material that came in contact with the water droplet re-dispersed as nanoparticles in the damaging water droplet, which resulted in drying behavior like the original polyester dispersion. The multiple ring patterns formed by polyester with moderate solubility may result from the imbalance between pinning and depinning dynamics due to fewer solid particles. The "gel pile" structure in case of least soluble polyester is a likely result of the poor penetration of water droplet through the polyester film.

AFM visualization revealed that as the film was deposited from the polyester dispersion, the nanoparticles fuse to form a continuous polyester film (Fig. S2, ESI†). Thermal treatment was required to prepare the original polyester dispersions in water from the bulk polyester resins. Therefore, it was expected that once the nanoparticles fuse together to form a continuous coating, they will not re-disperse in water without external energy input. However, when a water droplet was placed on the polyester film, the polyester nanoparticles re-dispersed spontaneously. The redispersion as nanoparticles of original size indicates that there may be residual trapped water in the film surrounding the nanoparticles. Due to having residual trapped water, polyesters with higher concentrations of ionic groups might be more susceptible to water damage. In contrast, polyesters with fewer ionic groups might undergo rapid interdiffusion of the hydrophobic groups which prevented penetration of water molecules in the film. Upon rapid heat treatment, the coatings' water resistivity dramatically improved for all studied polyester films except for the one with highest SSIPA content (Fig. 11). The heat treatment could have removed some, or all, of the residual water bound within the polyester film. Thus, nanofilms made from dispersions of polyesters with moderate fraction of hydrophilic groups can be efficiently rendered water-resistant by heat curing without further chemical crosslinking.[44]

Conclusions

We report data revealing some of the fundamental mechanisms of the formation and stability of waterborne sulfopolyester nanoparticle films. We fabricated nanofilms of brilliant structural colors in order to study and interpret the interaction of the nanofilms with water as a disruptive agent. The visualization and analysis of the structural color deriving from nanofilm thickness could be used as an effective experimental tool to test water resistivity and overall film integrity. Deposition of water droplets on such thin films resulted in spontaneous redispersion of the nanoparticles. Driven by convective flow,

water evaporation redistributed the polymer particles creating multiple colorful ring patterns. Using the color profile as a means to follow this polymer redistribution, we further explored the coffee-ring patterns as a function of the polymer composition, molecular weight, and electrolyte concentration. The degree of erosion was directly related to the fraction of hydrophilic monomer composition of the polyester, where more damage was induced for higher hydrophilic group content. Such coffee-ring erosion indicates possibility of damage to an uncrosslinked waterborne film by any aqueous environment. The results point out that this kind of water damage can be suppressed by molecularly designing polyesters with fewer hydrophilic groups. Our findings of the mechanisms of film formation by the waterborne polymer nanoparticles suggest how such environmentally friendly waterborne dispersions can be used in in applications such as optically clear or structurally colored coatings, paints, photonic paper and optical displays.

Experimental

Polyester dispersion

The polyester samples were provided by Eastman Chemical Company (Kingsport, TN). All experiments were carried out in deionized (DI) water from a Millipore Milli-Q system. Polyester dispersions in water were prepared by adding the measured amount of polyesters to hot DI water at 60–80 °C and allowing the dispersion to mix with active stirring for one hour. All sulfopolyesters readily dispersed in hot water except polyester 2, which required the addition of co-solvent *n*-propanol (0.38 g per g polyester) with extended heating and active stirring. The carboxylated polyester 9 required addition of volatile amine (dimethylethanolamine, DMEA) based on the acid number during the dispersing process. The pH of the dispersion of polyester 9 was maintained at 7.5. The volume of the dispersions was adjusted with DI water to obtain 30 wt% stock dispersions.

DLS measurements

The nanoaggregate polymer particle size was determined *via* DLS. The stock polymer dispersions (100 g L^{-1}) were diluted 3000× with DI water to eliminate the possibility of multiple scattering for DLS measurements. 1 mL of each diluted dispersion was transferred to a cuvette and measured in triplicate at 25 °C using a Zetasizer Nano ZSP (Malvern Instruments) with a 10 mW He–Ne laser at 633 nm and a photodiode located 173° from the incident laser beam. Plastic cuvettes were used for the measurements in water-based medium and glass cuvettes for organic solvents. The *Z*-average diameter and size distribution were measured by DLS using cumulant and distribution analysis algorithm respectively as described previously.[45]

Film formation and droplet test

Films were prepared by using convective assembly method as described previously.[30] In brief, 60 μL polyester dispersion (30 wt%) was injected between a horizontal and inclined plates. The inclination angle was close to 30°. The deposition speed was kept at 3.25 mL h^{-1} for all films. Ambient temperature (22–25 °C) and humidity (50–60% relative humidity) were maintained for all deposition condition. Silicon wafer (University Wafer, Inc., Boston, MA) was used as substrate. The wafers were subjected to standard cleaning with RCA method. The deposited coatings were allowed to dry at ambient conditions for one hour before the water droplet tests. For the droplet test, 1 μL water or other damaging liquid (salt or surfactant solutions) was dropped extremely carefully on the film and allowed to dry at ambient condition. For the heat curing experiments, the films were allowed to dry at 50 °C for 16 h before conducting droplet test with water.

Film characterization

The thickness of films was obtained using a spectroscopic ellipsometer from an average of 4–5 measurements (J.A. Woollam alpha-SE) at a fixed angle of 70°. The colors that were calculated from Bragg's law were directly correlated to the actual color of the films and the film thickness measured by ellipsometry. This direct comparison confirmed the origin of structural color based on constructive thin film interference. An error in this case could originate from the refractive index value obtained from the ellipsometry measurement, which however, was found to be very similar to the original refractive index of the polyesters. The camera was positioned to capture the images of the actual films at angles that were very close to 90°. However, if the camera was mounted at exactly 90° vertical position, then the films appeared gray (*i.e.*, the color of silicon wafers) due to the highly reflective property of silicon wafers. For obtaining the height profile of the erosion area, profilometry was performed with a Veeco Dektak 3 profilometer. AFM was utilized to check the surface topography of the polyester films with a Q-Scope 250 scanning probe microscope.

Conflicts of interest

There are no conflicts to declare.

Acknowledgements

The authors thank Eastman Chemical Company for financial and material support of this study. We also acknowledge support from NSF grants CBET-1604116 and CMMI-1825476. We thank Dr Scott George (Eastman Chemical Company) for synthesizing the polyesters and acknowledge Dr David Inglefield (Eastman Chemical Company) for fruitful discussions on the properties of polyesters. We also thank Yada Chulakham for assisting in making the dispersions and creating the nanofilms.

References

1 D. Dieterich, *Prog. Org. Coat.*, 1981, **9**, 281–340.
2 K.-L. Noble, *Prog. Org. Coat.*, 1997, **32**, 131–136.
3 A. Agirre, C. de las Heras-Alarcon, T. Wang, J. L. Keddie and J. M. Asua, *ACS Appl. Mater. Interfaces*, 2010, **2**, 443–451.

4 S. F. R. Tristram, C. J. Mason, J. M. Williams and D. B. G. Hinkley, *ChemSusChem*, 2015, **8**, 63–66.
5 Y. C. Tsai, S. Li, S. G. Hu, W. C. Chang, U. S. Jeng and S. H. Hsu, *ACS Appl. Mater. Interfaces*, 2015, **7**, 27613–27623.
6 C. W. Ou, C. H. Su, U. S. Jeng and S. H. Hsu, *ACS Appl. Mater. Interfaces*, 2014, **6**, 5685–5694.
7 S. Islam, D. L. Inglefield and O. D. Velev, *Soft Matter*, 2018, **14**, 2118–2130.
8 M. Goikoetxea, Y. Reyes, C. M. De Las Heras Alarcón, R. J. Minari, I. Beristain, M. Paulis, M. J. Barandiaran, J. L. Keddie and J. M. Asua, *Polymer*, 2012, **53**, 1098–1108.
9 J. A. McCaulley, K. A. Cox, S. W. Dobbs, S. E. George, E. E. McEntire and T. A. Oldfield, *J. Cosmet. Sci.*, 2009, **60**, 391–392.
10 A. F. Keddie and J. L. Routh, *Fundamentals of Latex Film Formation Process and Properties*, Springer, Dordrecht, 2010.
11 M. A. Winnik, *Curr. Opin. Colloid Interface Sci.*, 2010, **2**, 192–199.
12 P. A. Steward, J. Hearn and M. C. Wilkinson, *Adv. Colloid Interface Sci.*, 2000, **86**, 195–267.
13 C. Grüter, F. H. I. D. Segers, C. Menezes, A. Vollet-Neto, T. Falcón, L. Von Zuben, M. M. G. Bitondi, F. S. Nascimento and E. A. B. Almeida, *Nat. Commun.*, 2017, **8**, 195–267.
14 R. C. Satguru, R. McMahon, J. Padget and J. C. Coogan, *J. Coat. Technol.*, 1994, **66**, 47–55.
15 H. Cao, H. Noh, S. F. Liew, V. Saranathan, R. Prum, J. Forster, E. Dufresne and S. Mochrie, Cleo 2013, 2013, QW3A.1.
16 Z. Shen, Y. Yang, F. Lu, B. Bao and B. You, *Polym. Chem.*, 2012, **3**, 2495–2501.
17 N. Vogel, S. Utech, G. T. England, T. Shirman, K. R. Phillips, N. Koay, I. B. Burgess, M. Kolle, D. A. Weitz and J. Aizenberg, *Proc. Natl. Acad. Sci. U. S. A.*, 2015, **112**, 10845–10850.
18 V. L. Colvin, *MRS Bull.*, 2001, **26**, 637–641.
19 O. L. Pursiainen, J. J. Baumberg, H. Winkler, B. Viel, P. Spahn and T. Ruhl, *Opt. Express*, 2007, **15**, 9553.
20 Y. Kanamori, H. Katsube, T. Furuta, S. Hasegawa and K. Hane, *Jpn. J. Appl. Phys.*, 2009, **48**, 0–4.
21 H. Wang and K. Q. Zhang, *Sensors*, 2013, **13**, 4192–4213.
22 B. Tang, Y. Xu, T. Lin and S. Zhang, *J. Mater. Res.*, 2015, **30**, 3134–3141.
23 J. H. Holtz and S. A. Asher, *Nature*, 1997, **389**, 829–832.
24 F. Cheng, J. Gao, S. T. Luk and X. Yang, *Sci. Rep.*, 2015, **5**, 1–10.
25 L. Zulian, E. Emilitri, G. Scavia, C. Botta, M. Colombo and S. Destri, *ACS Appl. Mater. Interfaces*, 2012, **4**, 6071–6079.
26 Y. Ge, J. Goebl, J. He, L. Lu and Z. Yin, *Adv. Mater.*, 2009, **21**, 4259–4264.
27 H. Fudouzi and Y. N. Xia, *Langmuir*, 2003, **19**, 9653–9660.
28 O. Sato, S. Kubo and Z.-Z. Gu, *Acc. Chem. Res.*, 2008, **42**, 1–10.
29 Z. Gu, H. Uetsuka, K. Takahashi, R. Nakajima, H. Onishi, A. Fujishima and O. Sato, *Angew. Chem., Int. Ed.*, 2003, **42**, 894–897.
30 B. G. Prevo and O. D. Velev, *Langmuir*, 2004, **20**, 2099–2107.
31 Z. Shen, H. Chen and L. Wu, *Fabrication and Application of Structural Color Coatings*, John Wiley & Sons, Inc., 2015.
32 J. D. Forster, H. Noh, S. F. Liew, V. Saranathan, C. F. Schreck, L. Yang, J. C. Park, R. O. Prum, S. G. J. Mochrie, C. S. O'Hern, H. Cao and E. R. Dufresne, *Adv. Mater.*, 2010, **22**, 2939.
33 W. H. Bragg and W. L. Bragg, *X-rays and Crystal Structure*, G. Bell, London, 1915.
34 R. D. Deegan, O. Bakajin, T. F. Dupont, G. Huber, S. R. Nagel and T. A. Witten, *Nature*, 1997, **389**, 827–829.
35 D. Kaya, V. A. Belyi and M. Muthukumar, *J. Chem. Phys.*, 2010, **133**, 114905.
36 T. Still, P. J. Yunker, A. G. Yodh, D. Kaya, V. A. Belyi, M. Muthukumar, M. Anyfantakis, Z. Geng, M. Morel, S. Rudiuk and D. Baigl, *Langmuir*, 2010, **133**, 4984–4988.
37 T. Still, P. J. Yunker and A. G. Yodh, *Langmuir*, 2012, **28**, 4984–4988.
38 D. M. Kuncicky and O. D. Velev, *Langmuir*, 2008, **24**, 1371–1380.
39 B.-J. de Gans, P. C. Duineveld and U. S. Schubert, *Adv. Mater.*, 2004, **16**, 203–213.
40 P. J. Yunker, T. Still, M. A. Lohr and A. G. Yodh, *Nature*, 2011, **476**, 308–311.
41 H. Hu and R. G. Larson, *J. Phys. Chem. B*, 2006, **110**, 7090–7094.
42 Y. Li, Q. Yang, M. Li and Y. Song, *Sci. Rep.*, 2016, **6**, 1–8.
43 M. Anyfantakis, Z. Geng, M. Morel, S. Rudiuk and D. Baigl, *Langmuir*, 2015, **31**, 4113–4120.
44 J. Hu, K. Peng, J. Guo, D. Shan, G. B. Kim, Q. Li, E. Gerhard, L. Zhu, W. Tu, W. Lv, M. A. Hickner and J. Yang, *ACS Appl. Mater. Interfaces*, 2016, **8**, 17499–17510.
45 B. S. Mertens and O. D. Velev, *Soft Matter*, 2015, **11**, 8621–8631.

